RSS-Based DoA Estimation Using ESPAR Antennas and Interpolated Radiation Patterns

Lukasz Kulas, *Senior Member, IEEE*

***Abstract*—In this letter, it is shown how an algorithm, which employs received signal strength values in order to estimate direction of arrival (DoA) of impinging signals in wireless sensor network (WSN) nodes equipped with electronically steerable parasitic array radiator (ESPAR) antennas, can easily be improved by applying an interpolation algorithm to radiation patterns recorded in the calibration phase of the DoA estimation process. The proposed method allows one to measure ESPAR antenna's radiation patterns during the initial calibration phase with much coarser than 1° angular resolution, while the overall DoA estimation accuracy can be kept at the similar level. Measurements using a fabricated ESPAR antenna have indicated that anechoic chamber calibration procedure of WSN nodes equipped with such antennas can be done almost 50% faster, which in consequence will reduce system deployment costs in practical WSN applications where a number of WSN nodes can easily reach hundreds.**

***Index Terms*—direction of arrival (DoA), electronically steerable parasitic array radiator (ESPAR) antenna, interpolation algorithm, received signal strength (RSS), switched-beam antenna.**

I. Introduction

DIRECTION-OF-ARRIVAL (DoA) estimation using electronically steerable parasitic array radiator (ESPAR) antennas is an alternative approach to the one relying on antenna arrays with a number of digital signal processing (DSP) units [1]. A system employing many chains of DSP-based RF receivers can provide high-resolution DoA estimation of multiple signals without prior calibration [2]. However, it requires a number of DSP units that increase the overall costs and energy consumption.

As an alternative solution, ESPAR antennas are single-port output structures with only one active element surrounded by a number of parasitic elements, which are connected to reactances [3]–[6]. By setting such reactances to specific values, one can form a directional radiation pattern, and by changing these values electronically, one can also obtain different directions of the main beam [5], [6]. In practical system implementations, using ESPAR antenna beam-steering capability together with MUltiple SIgnal Classification (MUSIC) algorithm, one can estimate DoA of a signal impinging the antenna with 3° precision, which has been measured for an ESPAR antenna having six parasitic elements [6]. Further developments of the concept have led to a more practical DoA system implementation, free from accurate phase synchronization during signal measurements and high computational cost due to eigendecomposition required for the MUSIC algorithm [6], that relies on accurate measurements of the antenna's radiation patterns during the calibration phase and recorded received signal strength (RSS) values from an unknown target during DoA estimation [5]. For the same ESPAR antenna, DoA estimation can be performed with 0.67° estimation error mean and 2° precision using the power pattern cross-correlation (PPCC) algorithm introduced in [5]. One should note, however, that DoA estimation of multiple signals in RSS-based PPCC approach is much more challenging and limited than in methods relying on signal classification [2], [6].

Accurate RSS-based DoA estimation plays an important role in wireless sensor network (WSN) applications, in which, by equipping the nodes with reconfigurable antennas, one can improve connectivity, coverage, and energy efficiency of the whole network [7]. To this end, the PPCC concept has been adopted to WSN applications by introducing ESPAR antenna with simplified beam-steering circuit, which relies on RF switches providing required load to the parasitic elements (closed to open- or short-circuit) [8], rather than by applying correct bias voltages to varactor diodes [5], [6]. Such antenna can work with WSN nodes based on simple and inexpensive transceivers that can measure RSS of incoming packets.

The biggest drawback of the PPCC-based concepts is their lengthy calibration procedure, as in order to obtain accurate DoA estimations, one has to measure all ESPAR antenna's radiation patterns with at least 1° resolution. Such long calibration increases the time and associated costs required for system deployments, especially in practical WSN applications, in which the number of nodes can easily reach hundreds.

In this letter, a new PPCC-based DoA algorithm for ESPAR antennas is proposed and verified in measurements. The algorithm uses interpolated radiation patterns within PPCC estimator in a way easily applicable to practical realizations of WSN nodes, which commonly use inexpensive radio transceivers, equipped with ESPAR antennas. Measurement results indicate that the proposed concept reduces the time required for calibration in RSS-based DoA estimation, while keeping the overall accuracy at the similar level.

II. ESPAR Antenna Design and Realization

The proposed DoA estimation method relies on the ESPAR antenna concept with a simplified beam-steering, first proposed in [9], where instead of using varactors, four of five parasitic elements were soldered to the ground plane to provide directional

Manuscript received August 22, 2017; revised October 4, 2017; accepted November 2, 2017. Date of publication November 21, 2017; date of current version January 10, 2018. This work was conducted within the ENABLE-S3 project that has received funding from the ECSEL Joint Undertaking under Grant 692455. This Joint Undertaking receives support from the European Union's HORIZON 2020 research and innovation programme and Austria, Denmark, Germany, Finland, Czech Republic, Italy, Spain, Portugal, Poland, Ireland, Belgium, France, Netherlands, U.K., Slovakia, and Norway.

The author is with the Department of Microwave and Antenna Engineering, Faculty of Electronics, Telecommunications and Informatics, Gdansk University of Technology, Gdansk 80-233, Poland (e-mail: lukasz.kulas@eti.pg.gda.pl).

Digital Object Identifier 10.1109/LAWP.2017.2772043

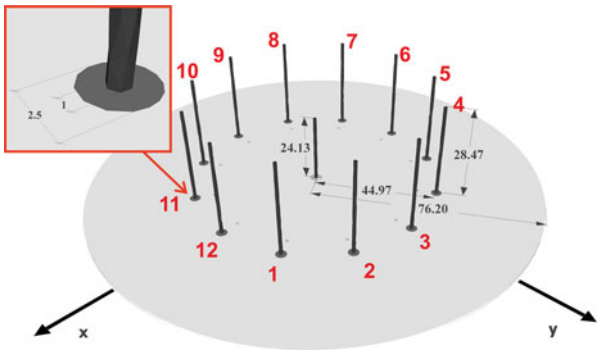

Fig. 1. Designed ESPAR antenna together with numbering of its parasitic elements. All the dimensions are in millimeters.

radiation pattern behavior. This approach has been successfully adopted to practical WSN applications to perform DoA estimation by using an ESPAR antenna [8], where one active monopole, fed by an SMA connector, is surrounded by 12 parasitic elements. In the antenna design, presented in Fig. 1, 1.7 mm height FR4 laminate with top-layer metallization as its ground plane has been used. Each of the parasitic elements can be connected to the ground or opened by a corresponding NJG1681MD7 SPDT (single-pole, double-throw) switch connected to the elements' ends at the bottom layer of the structure. Such a design, for which mathematical and physical reasoning is available in [3], [5], [9], and [10], allows one to control ESPAR antenna's radiation pattern electronically as every parasitic element connected to the ground, via its SPDT switch, becomes a reflector, while those opened become directors. Hence, the antenna's configuration can be denoted by the steering vector $V = [v_1, v_2, \ldots, v_{12}]$, where v_n denotes the state of each parasitic element: $v_n = 0$ for nth parasitic element connected to the ground and 1 for opened. In [8], it has been shown that such a design can easily be used in inexpensive WSN nodes, in which simple radio transceivers are commonly used, equipped with ESPAR antennas for providing efficient DoA estimation.

The ESPAR antenna has been designed in FEKO electromagnetic simulation software tool at the center frequency 2.484 GHz to obtain radiation patterns, presented in Fig. 2, with the narrowest directional main beam and also satisfactory antenna's input impedance matching. The initial antenna design from [8] has been optimized using the Simplex Nelder-Mead algorithm. By optimizing the distance between the parasitic elements and the active element, height of the active element, and height of the parasitic elements, it has been possible to maximize input impedance matching and to obtain maximum directivity of the directional beam. In consequence, for the final antenna dimensions, presented in Fig. 1, the input reflection coefficient equals -15.82 dB at the center frequency, while for the fabricated ESPAR antenna, shown in Fig. 3, the input reflection coefficient measured for all 12 configurations at 2.484 GHz is better than -14 dB.

III. DoA Estimation with Interpolated Radiation Patterns

The PPCC algorithm, proposed in [5] for DoA estimation, uses solely RSS values recorded at the ESPAR antenna's output, which makes the concept easily implementable in standard RF transceivers [8] that are commonly used in WSN nodes.

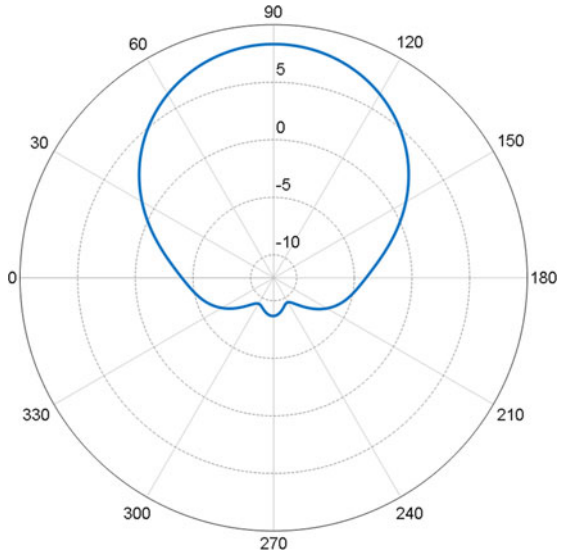

Fig. 2. Designed ESPAR antenna's horizontal plane radiation pattern (in dBi) providing directional main beam's direction $\varphi^1_{\max} = 90^\circ$ aligned with y-axis. The pattern has been obtained for $V^1_{\max} = [1, 1, 1, 1, 1, 0, 0, 0, 0, 0, 0, 0]$ (see text for explanations).

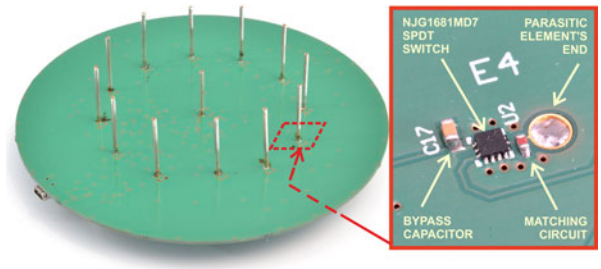

Fig. 3. Realized ESPAR antenna together with the SPDT switch connected to the fourth parasitic element's end at the bottom layer of the structure.

The algorithm relies on cross-correlation coefficient that is calculated between the antenna output recorded for different main beam directions and previously measured antenna's radiation patterns. For the proposed ESPAR antenna, the cross-correlation coefficient can be written in the following form:

$$\Gamma(\varphi) = \frac{\sum_{n=1}^{12} \left(P\left(V^n_{\max}, \varphi\right) Y\left(V^n_{\max}\right)\right)}{\sqrt{\sum_{n=1}^{12} P(V^n_{\max}, \varphi)^2} \sqrt{\sum_{n=1}^{12} Y(V^n_{\max})^2}} \quad (1)$$

where $\{P(V^1_{\max}, \varphi), P(V^2_{\max}, \varphi), \ldots, P(V^{12}_{\max}, \varphi)\}$ are ESPAR antenna's radiation pattern values for all corresponding steering vectors $\{V^1_{\max}, V^2_{\max}, \ldots, V^{12}_{\max}\}$ measured in an anechoic chamber once with the angular step precision $\Delta\varphi$ before the actual DoA estimation and $\{Y(V^1_{\max}), Y(V^2_{\max}), \ldots, Y(V^{12}_{\max})\}$ are output power values recorded during the actual DoA estimation process for a signal impinging the antenna from an unknown direction. Because the estimator $\Gamma(\varphi)$ is a correlation coefficient between $\{P(V^1_{\max}, \varphi), P(V^2_{\max}, \varphi), \ldots, P(V^{12}_{\max}, \varphi)\}$ and $\{Y(V^1_{\max}), Y(V^2_{\max}), \ldots, Y(V^{12}_{\max})\}$, the estimated DoA angle $\hat{\varphi}$ corresponds to the highest value of $\Gamma(\varphi)$ [5].

Since antenna's radiation patterns $P(V^n_{\max}, \varphi)$ in (1) are measured in an anechoic chamber with the angular step precision

$\Delta\varphi$ before the DoA estimation, they are in fact not continuous functions, but sets of discreet values. It means that, in practical implementations, we would rather use $\boldsymbol{p}^n = [p_1^n,\ p_2^n, \ldots,\ p_I^n]^T$ and $\boldsymbol{\varphi} = [\varphi_1,\ \varphi_2, \ldots,\ \varphi_I]^T$ to represent $P(V_{\max}^n,\ \varphi)$ and φ in a vector form. In consequence, to implement (1), one can rewrite it as

$$\boldsymbol{g} = \frac{\sum_{n=1}^{12} \left(\boldsymbol{p}^n\ Y\left(V_{\max}^n\right)\right)}{\sqrt{\sum_{n=1}^{12} \left(\boldsymbol{p}^n \circ \boldsymbol{p}^n\right)}\ \sqrt{\sum_{n=1}^{12} Y(V_{\max}^n)^2}} \tag{2}$$

where the symbol "$\circ$" stands for the Hadamard product, which is element-wise product of vectors, while $\boldsymbol{g} = [\Gamma(\varphi_1),\ \Gamma(\varphi_2), \ldots,\ \Gamma(\varphi_I)]^T$ is a vector of length I containing discretized values of the correlation coefficient $\Gamma(\varphi)$ associated with the corresponding discretized values of φ in the vector $\boldsymbol{\varphi}$. It means that by finding the highest value of $\boldsymbol{g}$ and the corresponding value in the vector $\boldsymbol{\varphi}$, one will simultaneously determine the estimated DoA angle $\hat{\varphi}$.

In the modified formulas of the cross-correlation coefficient (3), one can easily notice that the smaller the step $\Delta\varphi$ is, the finer representation of $\Gamma(\varphi)$ will be obtained. This is why accurate DoA estimations relying solely on RSS values require long calibration procedures, during which all ESPAR antenna radiation patterns are recorded with 1° resolution in the horizontal plane [5]. This effect is even more pronounced in WSN applications, in which, due to energy constrains, efficient simplified beam-steering is used [8], which requires higher number of radiation patterns to be used to maintain high DoA estimation accuracy. Long calibration procedure would then increase the time required for a system deployment in practical WSN applications, simultaneously influencing the associated costs, as in such applications the number of WSN nodes can easily reach hundreds.

In order to shorten the calibration procedure of an ESPAR antenna, we propose to use radiation patterns' interpolation to enhance PPCC method proposed in [5], which, thus far, has been used mainly to determine, based on two-dimensional (2-D) cuts provided by antenna producers, 3-D antenna radiation patterns in order to predict how electromagnetic wave will propagate [11]. It may be expected that, when antenna radiation patterns are measured with coarser $\Delta\varphi$ and the interpolation method used to refine measured radiation patterns after the calibration is accurate enough, the resulting DoA estimation accuracy could be close to the one obtained for fine ESPAR antenna radiation patterns measurements. Because, for radiation patterns $\boldsymbol{p}^n$ measured with the coarse angular step $\Delta\varphi$, associated interpolated radiation patterns $\tilde{\boldsymbol{p}}^n$ may easily be obtained, one can write (2) using interpolated radiation patterns in the following form:

$$\tilde{\boldsymbol{g}} = \frac{\sum_{n=1}^{12} \left(\tilde{\boldsymbol{p}}^n\ Y\left(V_{\max}^n\right)\right)}{\sqrt{\sum_{n=1}^{12} \left(\left(\tilde{\boldsymbol{p}}^n\right) \circ \left(\tilde{\boldsymbol{p}}^n\right)\right)}\ \sqrt{\sum_{n=1}^{12} Y(V_{\max}^n)^2}} \tag{3}$$

where $\tilde{\boldsymbol{g}} = [\Gamma(\tilde{\varphi}_1),\ \Gamma(\tilde{\varphi}_2), \ldots,\ \Gamma(\tilde{\varphi}_{\tilde{I}})]^T$ is a vector of length $\tilde{I}$ containing discrete values of the correlation coefficient $\Gamma(\varphi)$ associated with the corresponding values of φ in the vector $\tilde{\boldsymbol{\varphi}} = [\tilde{\varphi}_1,\ \tilde{\varphi}_2, \ldots,\ \tilde{\varphi}_{\tilde{I}}]^T$. Hence now, in order to estimate DoA angle, one has to determine the highest value of $\tilde{\boldsymbol{g}}$ and the corresponding value in the associated vector $\tilde{\boldsymbol{\varphi}}$.

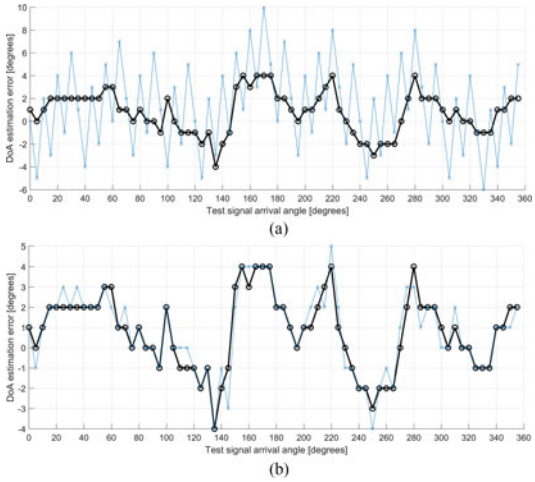

Fig. 4. DoA estimation error obtained from measurements at $\mathrm{SNR} = 20$ dB when different angular step precisions during calibration phase were used. The thick line with circle markers represents fine 1° resolution used in calibration phase, while the thin one represents DoA estimation errors for coarse 12° resolution used in fast calibration procedure (a) without and (b) with the proposed algorithm.

IV. Measurements

In order to verify the effectiveness and the overall accuracy of the proposed method, fabricated ESPAR antenna has been measured in our $11.9 \times 5.6 \times 6.0$ m anechoic chamber. During the calibration procedure, all 12 ESPAR antenna radiation patterns associated with 12 main beam directions have been measured at 2.484 GHz with eight different angular step precisions $\Delta\varphi = \{1°, 6°, 10°, 12°, 18°, 24°, 36°, 45°\}$. Then, to examine DoA estimation accuracy, a signal generator within NI PXIe-5840 Vector Signal Transceiver (VST) has been used to generate 10 dBm 2.484 GHz BPSK test signal impinging the ESPAR antenna. The signal source has been placed in the same anechoic chamber 8.0 m from the ESPAR antenna with the same NI PXIe-5840 VST connected to ESPAR antenna's output to receive the BPSK test signal. To make the results more realistic and easily comparable with those in [5] and [8], additive white Gaussian noise has been added to the received signal to generate a specific signal-to-noise ratio (SNR), and for every RSS measurement, ten snapshots were generated.

Signal's directions were chosen by rotating the receiving ESPAR antenna with a discreet angular step equal to 5° in the horizontal plane, which resulted in 72 test directions $\varphi_t \in \{0°, 5°, \ldots, 355°\}$. For every impinging signal's direction, 12 RSS values have been recorded for all the main beam antenna configurations $\{Y(V_{\max}^1),\ Y(V_{\max}^2),\ \ldots, Y(V_{\max}^{12})\}$, which are antenna output power values recorded for the corresponding steering vectors $\{V_{\max}^1,\ V_{\max}^2, \ldots, V_{\max}^{12}\}$.

To produce DoA estimation errors, for every considered SNR value, absolute values of estimation errors were calculated for all tested horizontal directions φ_t. From these 72 values, shown in Fig. 4 for $\mathrm{SNR} = 20$ dB and $\Delta\varphi = \{1°, 12°\}$, root-mean-square (rms) error and precision, which after [5] and [8] is the biggest absolute error value obtained during DoA estimation, have been calculated and gathered in Table I. In the results, it is clearly visible that by increasing the angular step $\Delta\varphi$, one can easily reduce the calibration time necessary to measure all 12 ESPAR antenna radiation patterns. However, without interpolation, it immediately affects the overall accuracy, which strongly declines as rms errors associated with DoA estimation increase

TABLE I
DoA Estimation Errors Obtained for the Proposed ESPAR Antenna With the Proposed PPCC Algorithm Involving Linearly Interpolated Radiation Patterns (See Text for Explanations)

				SNR = 20 dB		SNR = 10 dB		SNR = 5 dB	
	$\Delta\varphi$	no. of points	Calibration time [s]	rms	precision	rms	precision	rms	precision
without interpolation	**1°**	**360**	1994.32	2.00°	4°	2.10°	5°	1.93°	5°
	6°	**60**	1101.90	2.45°	5°	2.55°	6°	2.27°	5°
	10°	**36**	1030.49	3.54°	5°	3.54°	5°	3.73°	10°
	12°	**30**	1011.80	4.02°	10°	4.10°	10°	4.26°	10°
	18°	**20**	982.46	5.67°	11°	5.49°	11°	5.80°	11°
	24°	**15**	962.22	7.27°	15°	7.08°	13°	7.18°	14°
	36°	**10**	942.92	10.59°	20°	10.59°	20°	10.68°	20°
	45°	**8**	933.93	13.15°	25°	13.15°	25°	12.91°	20°
with linear interpolation	**1°**	**360**	1994.32	2.00°	4°	2.10°	5°	1.93°	5°
	6°	**60**	1101.90	2.03°	4°	2.05°	4°	1.95°	6°
	10°	**36**	1030.49	2.02°	4°	2.08°	5°	2.03°	6°
	12°	**30**	1011.80	2.10°	5°	2.09°	5°	2.00°	6°
	18°	**20**	982.46	2.17°	5°	2.12°	6°	2.09°	7°
	24°	**15**	962.22	2.15°	5°	2.30°	5°	2.14°	5°
	36°	**10**	942.92	2.55°	6°	2.64°	8°	2.89°	9°
	45°	**8**	933.93	4.06°	10°	4.08°	9°	4.05°	12°

for each SNR value. When interpolation is applied to produce interpolated radiation patterns $\tilde{\boldsymbol{p}}^n$ having 1° resolution from radiation patterns $\boldsymbol{p}^n$ measured with coarser angular step $\Delta\varphi$, the effect is not so severe anymore. Even for the simplest linear interpolation, which during the test has been calculated right after the calibration procedure, it is possible to obtain low rms errors for low numbers of calibration points. For $\Delta\varphi = 12^\circ$ and only 30 calibration points, the value of rms error increases by not more than 5% of the original value, which has been obtained for $\Delta\varphi = 1^\circ$ and 360 calibration points. Since the interpolation of radiation patterns $\tilde{\boldsymbol{p}}^n$ that have been calculated on Intel Core i7 2.6 GHz laptop right after the calibration procedure using a simple MATLAB code, which took 1.44 ms in the worst case when $\Delta\varphi = 45^\circ$, is very short, the calibration time is almost the same as for the corresponding coarser angular step calibration. It means that the calibration time of a single WSN node having DoA estimation capability can easily be reduced from 33 min and 14.32 s by approximately 49.27% with only negligible deterioration of the original DoA estimation performance. One should note, however, that although the proposed approach allows one to shorten the PPCC calibration, which has to be done only once, it does not affect the calculation time during DoA estimation phase. Hence, in order to additionally shorten the calculation time, one can apply a simplified version of the PPCC method proposed in [12].

V. Conclusion

In the letter, it has been shown how RSS-based DoA estimation algorithm for ESPAR antennas, which is used in WSN nodes in order to provide DoA estimation functionality, can be improved by employing interpolated radiation patterns. The proposed method allows one to measure ESPAR antenna's radiation patterns with coarser angular step $\Delta\varphi$, thus allowing for shorter anechoic chamber measurements of the antenna during the calibration phase of the PPCC-based DoA estimation algorithm. In order to verify the overall accuracy of the proposed method, the new approach has been applied to the fabricated ESPAR antenna with simplified beam switching, which can easily be integrated within a WSN node. Measurements indicate that, for the proposed algorithm, it is possible to estimate the direction of a signal impinging the antenna with similar rms errors and precisions but having only 30 calibration points per single radiation pattern, instead of 360 used when no interpolation of radiation patterns is applied. In consequence, the initial calibration time (more than 30 min) can be almost halved, while the overall DoA estimation accuracy stays almost at the same level.

References

[1] S. Chandran, *Advances in Direction-of-Arrival Estimation*. London, U.K.: Artech House, 2005.

[2] M. Donelli, F. Viani, P. Rocca, and A. Massa, "An innovative multiresolution approach for DOA estimation based on a support vector classification," *IEEE Trans. Antennas Propag.*, vol. 57, no. 8, pp. 2279–2292, Aug. 2009.

[3] R. Harrington, "Reactively controlled directive arrays," *IEEE Trans. Antennas Propag.*, vol. AP-26, no. 3, pp. 390–395, May 1978.

[4] M. Rzymowski, P. Woznica, and L. Kulas, "Single-anchor indoor localization using ESPAR antenna," *IEEE Antennas Wireless Propag. Lett.*, vol. 15, pp. 1183–1186, 2016.

[5] E. Taillefer, A. Hirata, and T. Ohira, "Direction-of-arrival estimation using radiation power pattern with an ESPAR antenna," *IEEE Trans. Antennas Propag.*, vol. 53, no. 2, pp. 678–684, Feb. 2005.

[6] E. Taillefer, C. Plapous, J. Cheng, K. Iigusa, and T. Ohira, "Reactance-domain MUSIC for ESPAR antennas (experiment)," in *Proc. IEEE Wireless Commun. Netw. Conf.*, New Orleans, LA, USA, Mar. 2003, vol. 1, pp. 98–102.

[7] F. Viani, L. Lizzi, M. Donelli, D. Pregnolato, G. Oliveri, and A. Massa, "Exploitation of parasitic smart antennas in wireless sensor networks," *J. Electromagn. Waves Appl.*, vol. 24, no. 7, pp. 993–1003, Jan. 2010.

[8] L. Kulas, "Direction-of-arrival estimation using an ESPAR antenna with simplified beam-steering," in *Proc. 47th Euro. Microw. Conf.*, Nuremberg, Germany, 2017, pp. 296–299.

[9] R. Schlub and D. V. Thiel, "Switched parasitic antenna on a finite ground plane with conductive sleeve," *IEEE Trans. Antennas Propag.*, vol. 52, no. 5, pp. 1343–1347, May 2004.

[10] T. Hassan, A. Kausar, H. Umair, and M. A. Anis, "Gain optimization of a seven element ESPAR Antenna using quasi-Newton method," in *Proc. IEEE Int. Conf. Microw. Technol. Comput. Electromagn.*, Beijing, China, 2011, pp. 293–296.

[11] F. Mikas and P. Pechac, "The 3D approximation of antenna radiation patterns," in *Proc. Inst. Elect. Eng. 12th Int. Conf. Antennas Propag.*, 2003, pp. 751–754.

[12] Y. Ozaki, J. Ozawa, E. Taillefer, J. Cheng, and Y. Watanabe, "A simple DOA estimator using adjacent pattern power ratio with switched beam antenna," *Prog. Electromagn. Res. C*, vol. 22, pp. 55–71, 2011.